Available online at www.sciencedirect.com

SCIENCE DIRECT®

Journal of the European Ceramic Society 25 (2005) 1109–1118

www.elsevier.com/locate/jeurceramsoc

Dispersion of alpha-alumina ultrafine powders using 2-phosphonobutane-1,2,4-tricarboxylic acid for the implementation of a DCC process

A.-L. Penard, F. Rossignol*, H. S. Nagaraja, C. Pagnoux, T. Chartier

SPCTS, CNRS-UMR 6638, ENSCI, 47 à 73 Avenue Albert Thomas, 87065 Limoges, France

Received 8 January 2004; received in revised form 23 April 2004; accepted 1 May 2004

Abstract

In this paper, we compare the effectiveness of 2-phosphonobutane-1,2,4-tricarboxylic acid (PBTCA) with that of 4,5-dihydroxy-1,3-benzene-disulfonic acid (Tiron) as electrostatic dispersants for concentrated alpha-alumina ultrafine powder suspensions. Three grades of alpha alumina powders with diameters in the range of 100–300 nm are tested. The comparison based upon direct measurements of electrokinetic properties, adsorption isotherms and rheology shows that both PBTCA and Tiron are good candidates for dispersion. In addition, the method of adsorption of PBTCA and Tiron onto the alumina surface is described. Like Tiron, PBTCA is adsorbed as a monolayer through an inner sphere complex. The key contribution of the phosphonate foot of the PBTCA molecule in the adsorption mechanism is demonstrated and the influence of alumina surface chemistry, especially hydroxylation, on adsorption is pointed out. Finally, it is shown that the concentrated suspensions could be used to implement a shaping process by direct coagulation casting (DCC).

Keywords: Suspensions; Shaping; Direct coagulation casting; Alumina ultrafine powders; Al_2O_3

1. Introduction

It is now well established that one can derive benefit from the intimate structure of ceramics at the low scale.[1] If fine microstructures can be associated with critical flaws of small sizes, this may lead to improved mechanical properties, i.e. higher Weibull modulus and higher rupture strength. The fracture toughness may also be increased depending on the grain aspect ratio and grain boundary composition that control to a large extent the sub-critical crack growth.[2] Nevertheless, even if many kinds of ultrafine powders are now commercially available at affordable costs, the major industrial challenge remains the fabrication of 3D parts of large dimensions and complex shapes with such powders. Researchers are still facing two difficulties: (i) the shaping and (ii) the densification.

(i) Traditional shaping methods are often not adapted to the specificity of ultrafine powders. In particular, ultrafine powders are strongly agglomerated because of Van der Waals forces, and the removal of agglomerates is essential for obtaining *defect-free* granular compacts prior to sintering. Wet dispersion is probably the preferential route used in this aim,[3,4] although high solid loadings are difficult to get. As a result, significant shrinkage and cracking may occur during the drying stage or the sintering stage. Similarly, dry processes, like Cold Isostatic Pressing, are difficult to implement. In this case, each contact between the ultrafine particles generates a force opposed to the compaction, and the smaller the particles are, the higher the number of contacts there are.

(ii) The densification ability and the homogeneity of the microstructure are closely related to the particle packing after shaping.[5] A higher degree of particle coordination in green bodies obviously helps with densification by matter transfer, but, in parallel it can also promote grain growth. For alumina materials, this grain growth tends to be abnormal and a drastic decrease of mechanical properties happens. When working on alumina, Krell et al.[6]

---

* Corresponding author. Tel.: +33 5 55 45 22 60; fax: +33 5 55 79 09 98.

E-mail address: f_rossignol@ensci.fr (F. Rossignol).

0955-2219/$ – see front matter. © 2004 Elsevier Ltd. All rights reserved.
doi:10.1016/j.jeurceramsoc.2004.05.006

> recently demonstrated that neither sintering nor the choice of the finest raw powders are the main features to obtain submicrometer ceramics. They argued that inter-particle forces lead to local agglomeration which counters densification and compensates for the increased diffusion. They then concluded that the particle homogeneity of the shaped green bodies was the key point.

New shaping methods based on colloidal processing, such as gel casting (GC)[7,8] or direct coagulation casting (DCC),[9,10] have recently emerged to respond to the implicit requirements of reproducibility and reliability linked to the development of dense ceramics with very fine microstructures. GC involves pouring a concentrated suspension of ceramic powder mixed with an organic monomer solution into a nonporous mold. Then, the monomer undergoes in situ polymerization giving rise to a consolidated body that adopts the shape of the mold. One major drawback of GC is the fact that the steric barriers generated by polymers between particles limit the solid loading. That is why, DCC, which does not use polymeric additives, appears so promising. The DCC basic principle is to coagulate a stable concentrated suspension poured into a nonporous mold by using a time-delayed chemical reaction. The destabilization is usually the result of an increase in the ionic strength that can be accompanied with a variation in the pH towards the isoelectric point (IEP). High solid loadings lead to highly homogeneous dense green bodies, with negligible linear shrinkage occurring during the liquid to solid transition and during the drying stage. Components with accurate sizes and complex shapes have been obtained by DCC.

In this paper, our goal is to prepare concentrated alumina suspensions that could be suitable for the further implementation of a DCC process. We discuss the aqueous dispersion ability of three kinds of alpha-alumina ultrafine powders with diameters slightly above 100 nm. The potential of 2-phosphonobutane-1,2,4-tricarboxylic acid (PBTCA) as an additive for electrostatic stabilization has been first recognized by Liu et al.[11] and later by Studart et al.[12] The PBTCA effectiveness is here compared to that of Tiron which has already been demonstrated.[13] The comparison is based on direct measurements of electrokinetic properties, adsorption isotherms and rheology. The dispersion mechanisms, especially the grafting of the additives on the alumina surface, as well as the role of the alumina surface chemistry, are described. Finally, it is shown that PBTCA could be an alternative to Tiron in achieving highly concentrated and stable suspensions of alumina ultrafine powders for the implementation of a DCC process. As an illustration, preliminary results on a possible DCC route are given showing the relationship of the present state of fundamental research to the targeted application.

2. Experimental procedure

2.1. Starting materials

Three types of alpha-alumina raw ultrafine powders are tested: two batches termed AKP30 and AKP50 supplied by Sumitomo Chemical Co. (Osaka, Japan) and one batch termed B15CR and numbered 12783 supplied by Baikowski SA (Annecy, France). The B15CR grade corresponds to a B15 powder which has been treated by air jet to remove hard agglomerates. All of the as-mentioned powders are high purity grades suitable for *bio* applications. It should be noted that we consider the AKP30 as a reference because of the comprehensive data already published on it.[10,13]

The main features of the ultrapure alpha-alumina ultrafine powders we study are reported in Table 1. We indicate in parentheses the results of our own measurements (N_2 BET and laser granulometry with a Mastersizer 2000 from Malvern Instruments). These results are in good agreement with the manufacturers specifications, also given in the table. The AKP30 is the coarsest powder and it exhibits an average diameter twice that of the B15CR powder, i.e. 0.32 μm, and a BET surface area half that of the B15CR powder, i.e. 7 $m^2\ g^{-1}$. The AKP50 characteristics are just in between that of AKP30 and B15CR. In addition, the AKP grades show a morphology that is more equiaxe than that of the B15CR (Fig. 1). The specific morphology of B15CR also explains why its BET surface area is larger.

Table 1
Main features given by suppliers of alumina ultrafine powders used in the present work

Qualitative data	Grade		
	AKP-30 (*Sumitomo*)	AKP-50 (*Sumitomo*)	B15CR (*Baikowski*)
Crystal form	α	α	α
Purity (%Al_2O3)	>99.99	>99.99	∼100
Ultimate Particle size (μm)	∼0.3 ($d_{50} = 0.32$)	0.1–0.3 (d_{50} = O.24)	∼0.15 ($d_{50} = 0.17$)
BET surface area (m^2/g)	5–10 (7)	9–15 (11)	15 (14)
Impurity level Si (ppm)	≤40	≤25	100
Na (ppm)	≤10	≤10	35
Fe (ppm)	≤20	≤20	3
Mg (ppm)	≤10	≤10	<20
Cu (ppm)	≤10	≤10	<20

Parentheses outline our own measurements.

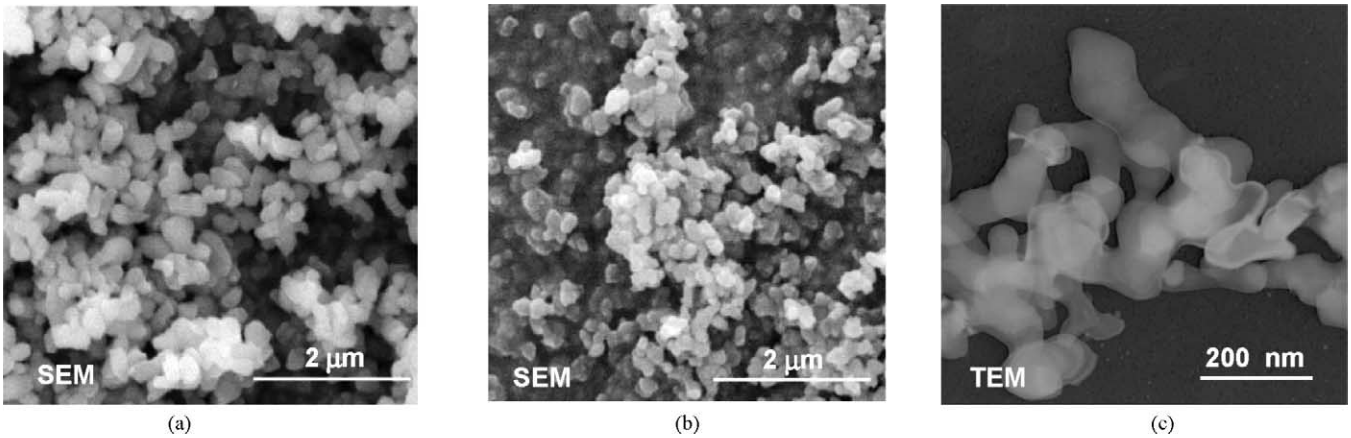

Fig. 1. SEM and TEM images of the different ultrafine powders: (a) AKP30, (b) AKP50, (c) B15CR.

2.2. Dispersion procedure

The powder dispersion is performed in deionized water. The desired water pH is adjusted using HCl for acidic pH or NaOH for basics. The ionic strength is fixed using NaCl salt. 2-Phosphonobutane-1,2,4-tricarboxylic acid (PBTCA) is introduced as a dispersant agent in the form of a sodium salt (PBTCA-Na_4 from Bayer). Its effectiveness is compared to that of 4,5-dihydroxy-1,3-benzenedisulfonic acid (Tiron from Aldrich) added as a disodium salt, and which has already been described in detail.[10,13]

All the suspensions used in this study are prepared according to the same procedure. First, the desired amount of dispersant is dissolved in water. The amount of dispersant is calculated in mol m^{-2} of the total surface area of the alumina particles to be introduced. The alumina powders are then added to the water-based solution and a strong ultrasonic treatment (pulsed, 3 min, 600 W-Vibra-cell ultrasonic desintegrator VC 600, Sonic and Materials, USA) is applied to break down the agglomerates. When it is necessary to reach large concentrations (i.e. over 50 vol.%), the powders are added to the liquid in several stages, with each stage being separated by a period of ultrasonic treatment. Finally, in order to reach a chemical equilibrium, suspensions are stabilized for at least 12 h with a low-speed rotating roller.

2.3. Rheological behavior

The rheology of suspensions containing 50–55 vol.% of dry matter depending on the type of powders is studied using a controlled stress rheometer (Carrimed, CSL 100). A trap is used to avoid solvent evaporation and a cone-plane configuration is used for the following reasons: (i) the shear rate is uniform on the whole plane, so that the result is representative of the entire sample, (ii) a very low amount of suspension is required (<2 ml). Considering our suspensions rheology range, a 4 cm–2° assembly is chosen. The experiment is done at room temperature, and the procedure is as follow. A pre-stress of 10 N m^{-2} is applied for 10 s to give the same *history* to each sample. Then, a waiting time of 10 s allows the stabilization of the system. Finally, a linearly increasing shear stress (τ) from 0 to 50 N mm^{-2} is applied as a function of time and the resulting evolution of the shear rate ($\dot{\gamma}$) is measured typically up to 250 s^{-1}. The consistency (K in Pa s^n) is calculated with the Herschel–Buckley model often used to describe the rheology of concentrated ceramic suspensions, i.e.

$$\tau = \tau_0 + K\dot{\gamma}^n \tag{1}$$

where τ_0 is the threshold shear rate (yield value), n the shear rate index. We consider that the best state of dispersion is obtained for a minimum value of K.

2.4. ESA measurements

The zeta potential of the dispersed particles is determined by an Electrokinetic Sonic Amplitude (ESA) technique with a Model ESA8000 from Matec (Northborough, MA, USA). The measurements are carried out with slurries loaded at 3.3 vol.% of solid. The ionic strength is fixed at 10^{-2} mol L^{-1} by NaCl addition. In order to cover a wide range of pH, two suspensions are prepared for each slurry composition. One is used to determine the ESA signal from natural to acidic pH and the other one for basics. The ESA probe is calibrated with an aqueous suspension of 10 vol.% of Ludox TM from Du Pont (Wilmington, DE, USA). In this paper, since ESA signals are directly proportional to the electrophoretic mobilities of the particles (i.e. zeta potential), they have been chosen to be representative of the variation of electrokinetic properties versus pH.

2.5. Adsorption isotherms

The PBTCA and Tiron adsorption isotherms are plotted for a given pH as a function of the amounts of dispersant/square meter of added powder. Slurries are prepared with 3 vol.% solid loading. The solvent is an aqueous solution of NaCl (10^{-2} mol L^{-1}) used to fix the ionic strength. The pH is adjusted using HCl and NaOH solutions. After 12 h of stabilization, the supernatant is removed using a centrifuge and the quantity of non-adsorbed molecules contained in the supernatant is determined by observing the phosphorous atoms using ICP (IRIS apparatus from ThermoOpteck, UK). The adsorbed amount of dispersant is calculated from the difference between the initial quantity added and that remaining in the supernatant.

3. Results and discussion

3.1. Dispersants

The molecular configurations of the additives used for dispersion, PBTCA and Tiron, have been calculated using Chem3D from CambridgeSoft (Fig. 2). It is to be noticed that the acidic form of PBTCA has been represented instead of the tetrasodium salt. For PBTCA, the three carboxylic groups attached to the butyl chain are constituting a *pseudo* 2D layer, which is supported by a phosphonate foot extending in a direction perpendicular to the layer. The idea of testing PBTCA as a dispersant for ceramics should be attributed to Liu et al.[11,14–16] It comes from the fact that this molecule can be used for water treatment,[17] since it is known to form complexes with several metal cations like Ca^{2+}, Mg^{2+}, Al^{3+} or Fe^{3+} through the phosphonate foot. In fact, the PBTCA molecule looks very much like a flexible *umbrella* that could be included in a rectangle parallelepiped whose volume would be roughly 0.2 nm^3. In principle, PBTCA exhibits five ionizable sites (pK_a: 3.74, 4.23, 5.14, 6.8, 9.05). However, the PBTCA salt used in this study contains only 4 sodium (PBTCA-Na_4). The acidic site which is not coordinated with a sodium cation is an hydroxyl one that stands in the neighborhood of the phosphorous atom. Although the PBTCA molecule is very small, it looks a bit like acrylic-based polymers (PAAs) with respect to the presence of mostly carboxylic groups. When dissociated to form neg-

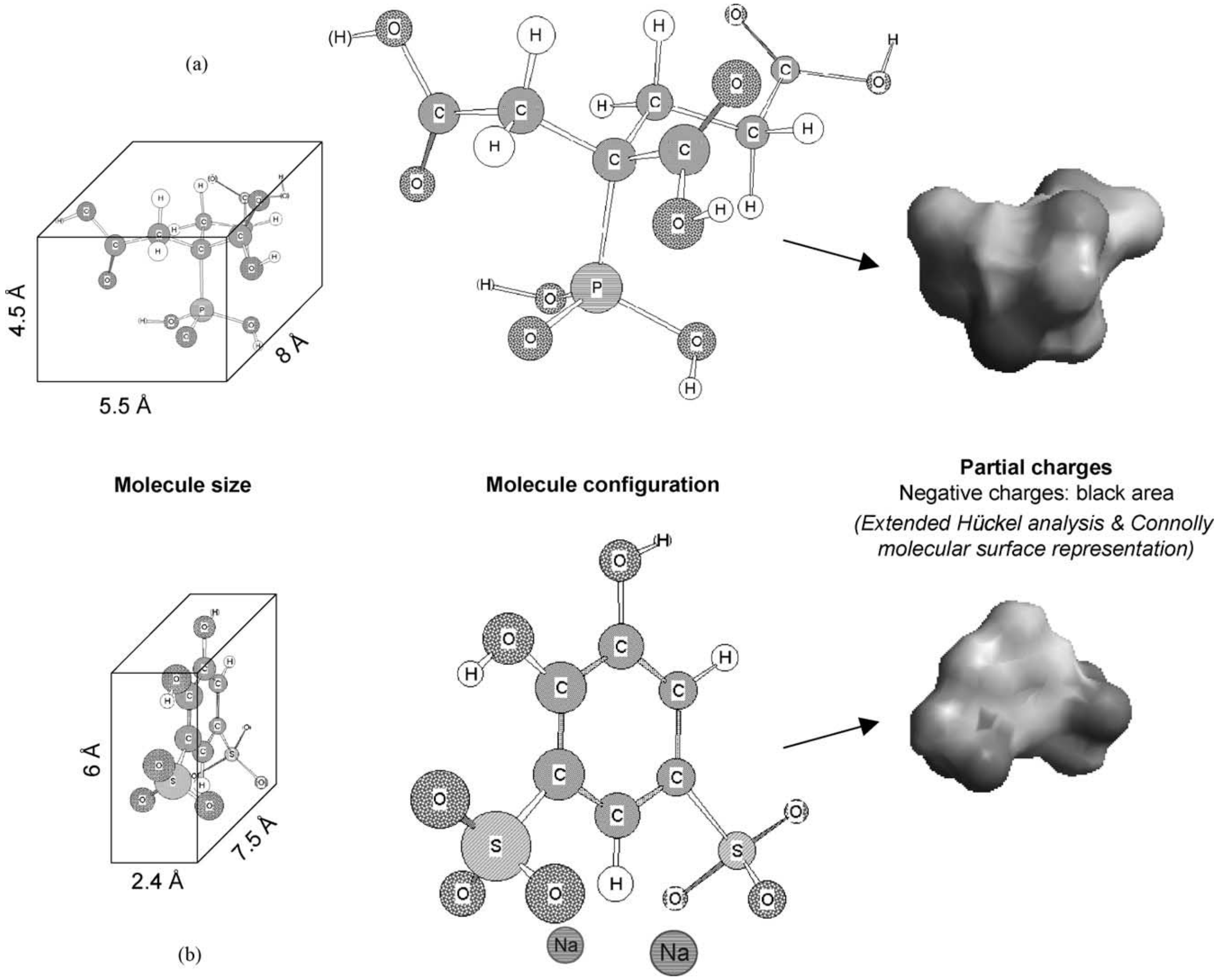

Fig. 2. Chem3D modelling of PBTCA (a) and Tiron (b) configuration and partial charges.

atively ionized polyelectrolytes, PAAs are commonly used as dispersants providing enhanced stability via electrosteric forces.

Tiron is a weak tetraprotic acid which corresponds to two hydroxylic and two sulfonic groups attached to a benzene ring giving rise to a more rigid structure than that of PBTCA. The third and fourth pKa values associated with the hydroxylic acid sites are 7.20 and 11.8. Tiron forms chelates with a large number of metal ions including Al^{3+} by stepwise proton transfers on the OH groups. Consequently, it is not surprising to observe that Tiron can easily be grafted onto alumina surface by creation of an inner sphere complex.[13,18] However, in this specific case, it is likely that Al-hydroxide complexes form instead of true free Al^{3+}complexes, because of the hydroxylation of alumina surfaces in water. At the opposite, the sulfonic acid sites easily give up their protons, which results in very low pK values, and are therefore generally not reported. The sulfonic groups carry the charge when Tiron is grafted onto alumina leading to an electrically negative particle surface suitable for good dispersion ability. At the same time, Na^+ cations coordinate around complexes to help stabilize them. Finally, we would like to point out two interesting features of the Tiron molecule. Firstly, it is twice as small (volume of about 0.1 nm^3) as PBTCA and highly symmetrical, especially with respect to the plane of the benzene ring. Secondly, such a rigid molecule, derived from catechol, is very adaptable because of the possibility to change the number and/or type of functional groups attached to the benzene ring in order to significantly modify the dispersion properties.[13,19]

3.2. *Powder deagglomeration*

Most of the time, the ultrafine powders are strongly aggregated, as well as agglomerated, under the influence of Van Der Waals forces. Obtaining true isolated single particles therefore becomes a key point to implement successful shaping processes. In Fig. 3, we have reported the size distributions of the three grades of alumina ultrafine powders before and after dispersion with ultrasounds (see Section 2.2). Before dispersion, two populations of particles are observed whatever the ultrafine powders examined (Fig. 3a). The larger diameter population lies in a range from 10 to 100 μm and may correspond to soft agglomerates, since it easily disappears after dispersion (Fig. 3b). The second population between 1 and 10 μm most likely results from strong aggregates that are difficult to break by ultrasonic treatment, for the two AKP grades. Indeed, after dispersion, a *residue* is still present from 1 to 10 μm for the AKP ultrafine powders, whereas it is not observed for B15CR. It indicates that the air jet deagglomeration pretreatment performed by the B15CR supplier is efficient. Finally, gaussian peaks appearing after dispersion in a range of 0.08–0.8 μm would therefore correspond to elementary particles.

3.3. *Optimum concentration of dispersant*

An important step in the DCC shaping process involves obtaining concentrated suspensions with a low consistency together with a high solid loading, which is in itself contradictory. We consider that the optimum dispersant concentration is the one which leads to the best state of dispersion, i.e., to a minimum consistency (*K*, Eq. (1)). The Fig. 4a and b show the evolution of consistency at natural pH (i.e. pH around 8–9) with respect to PBTCA and Tiron concentrations. It should be noticed that the consistency values for the three grades of alumina ultrafine powders are not directly comparable because they are obtained at different solid loadings. For solid loadings higher than the ones noted in Fig. 4a and b, the consistency values are too high to obtain a good comparison of dispersant effectiveness. This is actually the result of different dispersion abilities of our ultrafine powders in relationship with the electrostatic charge developed onto their surface, as demonstrated in Section 3.4.

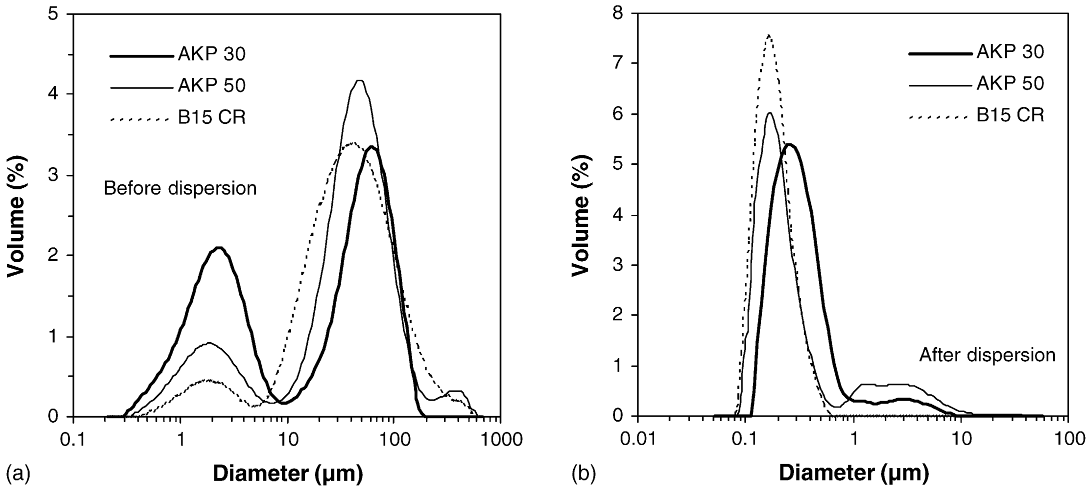

Fig. 3. Size distribution of alumina ultrafine powders before (a) and after (b) dispersion by ultrasounds in the presence of Tiron.

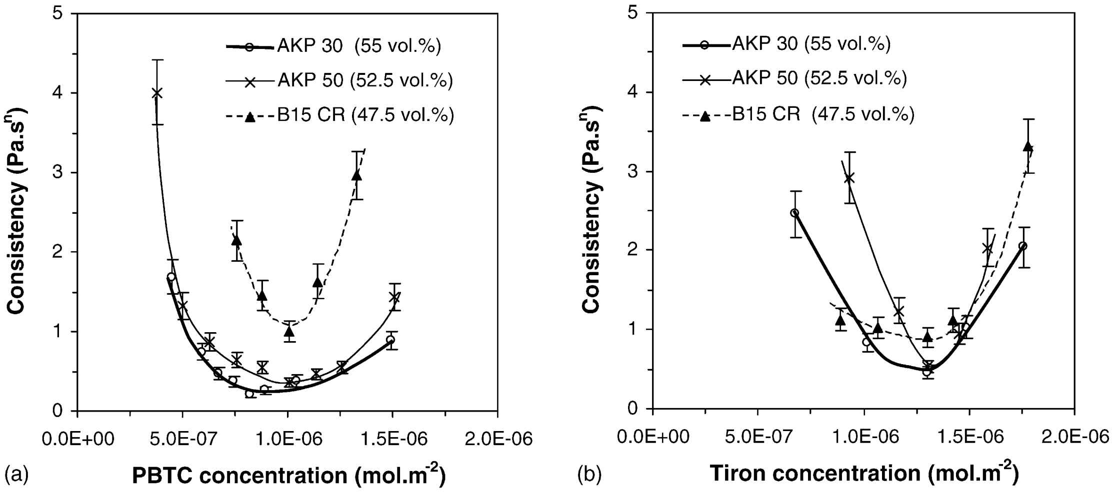

Fig. 4. Consistency of concentrated suspensions in the presence of PBTCA (a) and Tiron (b).

When dispersants are added to suspensions, the consistency initially decreases down to a minimum value as a result of stabilization. The minimum consistency corresponds to maximum stabilities and optimum concentrations of dispersants. The minimum consistency reached for a given powder is close whatever the type of dispersant used, indicating that PBTCA is as efficient as Tiron. Moreover, for a given dispersant, optimum concentrations are constant whatever the type of powder. This optimum concentration is $1 \times 10^{-6}\,\mathrm{mol\,m^{-2}}$ for PBTCA (Fig. 4a) and $1.3 \times 10^{-6}\,\mathrm{mol\,m^{-2}}$ for Tiron (Fig. 4b), respectively. The lower value observed for PBTCA could be simply attributed to the specific morphology of PBTCA molecule (i.e. greater size, *umbrella* shape) conferring a better ability to cover surfaces. Some chemical phenomena related to the grafting mechanism of dispersants itself may also contribute to modify the value of the optimum concentration. It depends on the nature of functional groups of dispersants used and the density of available adsorption sites on the surface of a given alumina powder. For larger amounts of added dispersant, non-adsorbed molecules induce a higher ionic strength, and hence a destabilization of the suspension, that leads to an increase of consistency.

3.4. *Electrostatic charging of alumina surface*

The variation of the ESA signal is measured as a function of pH with no additives (Fig. 5a) and for the optimum concentrations of PBTCA (Fig. 5b) and Tiron (Fig. 5c), respectively. When no additives are used, the isoelectric points (IEPs) are close to pH 9 (Fig. 5a) in agreement with the fact that the AKPs and the B15CR are high purity powders. Moreover, the AKPs exhibit almost identical ESA curves, whereas the electrostatic charging of B15CR, especially below the IEP, is lower. Although the main features of ultrafine powders are similar (Table 1), the different fabrication processes of Sumitomo and Baikowski probably lead to surface chemistries that vary.

The effectiveness of an electrostatic dispersant is related to its capability to generate a high surface charge, whether positive or negative, in the working conditions in term of pH, i.e. to shift the IEP as far as possible. In principle, the higher the absolute value of the charge, the better the stability will be. Fig. 5b and c allow the comparison of the effectiveness of PBTCA and Tiron. A stabilization with negative charges is achieved with both dispersants at the natural pH (i.e. pH around 8–9) of alumina. For a given powder, the maximum negative charge reached is similar with PBTCA and Tiron. In addition, for both dispersants, a slightly higher ESA signal is obtained with AKP30 compared to AKP50 and B15CR, with the results for the last two powders being comparable. As a result, we effectively observe that it is easier to reach high solid loading (>55 vol.%) with AKP30. On the other hand, even if the maximum negative charges reached with AKP50 and B15CR are equivalent, there is a higher consistency for the B15CR concentrated suspensions (Fig. 4), confirming the fact that the morphology of the powders also greatly influences the rheological properties at high solid loadings, i.e. particles almost in contact.

The IEPs decrease down to lower pH values together with dispersant additions, but a better surface covering is observed outside the optimum of consistency only with PBTCA (Fig. 6). When considering the optimum concentrations of dispersants determined from consistency measurements, we observe that the IEPs are shifted towards pH 2–3 for Tiron (Fig. 5c), but only towards pH 3–5 for PBTCA (Fig. 5b) because of the neutralization of all carboxylic groups at pH below 4. Dispersions prepared with Tiron are stable over a larger range of pH (from pH 7–11) than those prepared with PBTCA (pH from 8 to 10). Above pH 12, the drastic decrease of ESA signals in term of absolute value, is consequent on the desorption of dispersants. In conclusion, the PBTCA effectiveness as dispersant at natural pH is comparable to that of Tiron whatever the powders, but the reduced stability range it induces will probably make

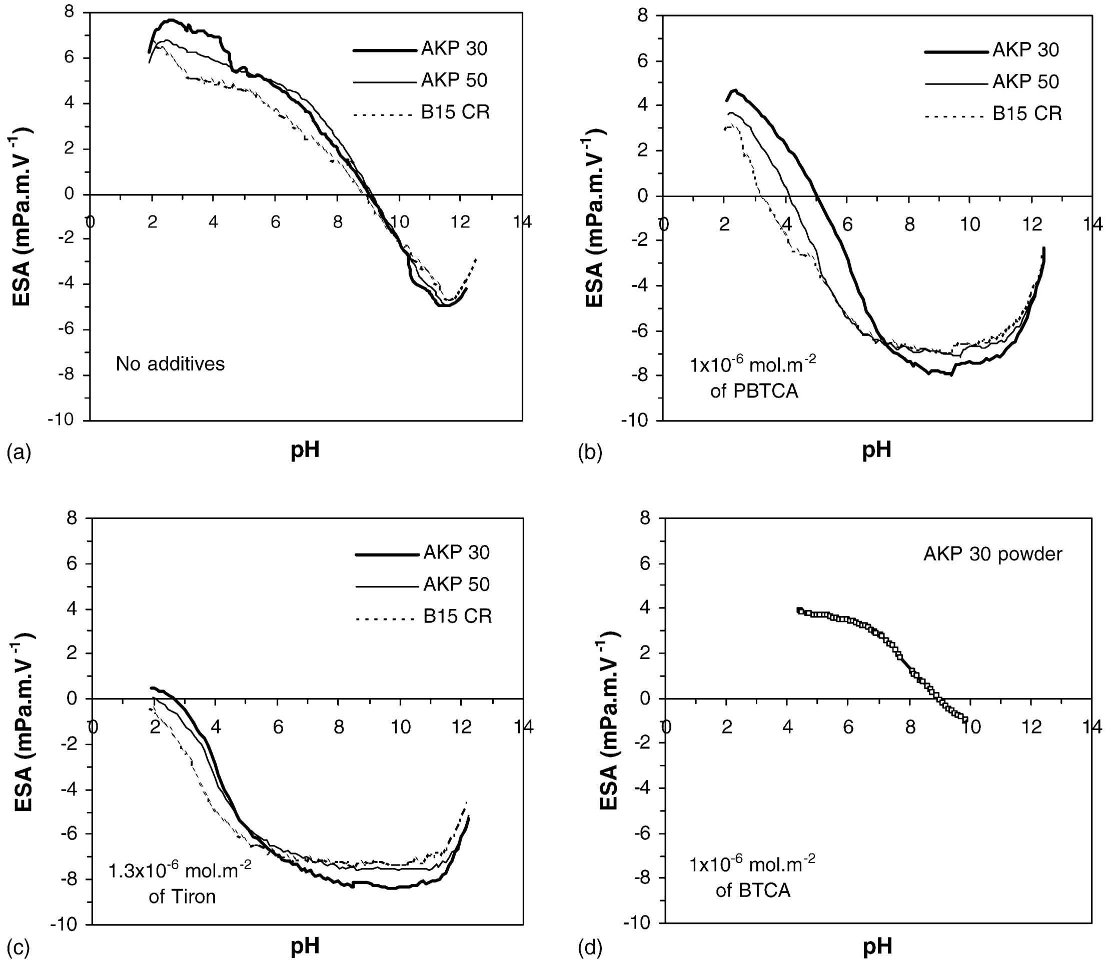

Fig. 5. ESA data vs. pH with no additives (a) and with optimum concentrations of PBTCA (b), Tiron (c), and BTCA (d).

the coagulation by pH shift easier. That constitutes an advantage for the implementation of a reliable DCC process.

The adsorption mechanisms of dispersants depend a lot on the hydroxylation of alumina surfaces (Al–OH sites). A fraction of the Al–OH groups present at the alumina surface in water are dissociated upon acido-basic equilibria into Al–OH_2^+ or Al–O^-. For the sake of clarifying, we assume that Al–OH_2^+ and Al–O^- are the only existing charged species, although other species may be encountered. The ratio between positive and negative species gives the sign and the intensity of the surface charge. Without additives, all powders are slightly positively charged (Fig. 5a) at natural pH (i.e. pH 8), indicating that there are more Al–OH_2^+ than Al–O^- sites on the surface. Actually, the site density depends on the polarization generated by counterions (i.e. Na^+), the crystalline structure of alumina and the powder synthesis process. The Sumitomo and Baikowski synthesis processes being different likely lead to different surface chemistries as well.

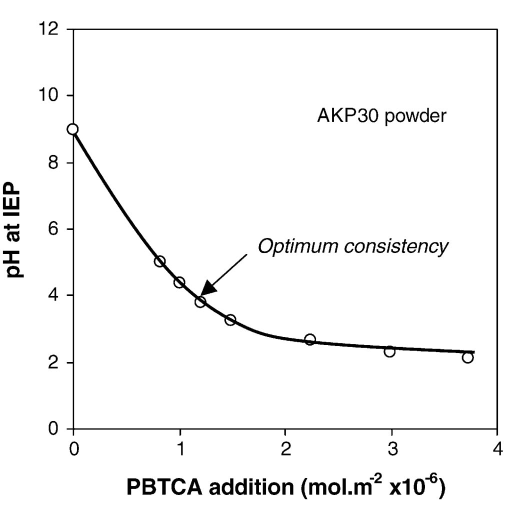

Fig. 6. Evolution of pH at the IEP together with PBTCA addition into an AKP30 suspension.

The powders become negatively charged as a result of the dispersant grafting. The negative electrostatic charging is due to ionized functional groups that are mainly COO^- for PBTCA and SO_3^- for Tiron. The effectiveness of a dispersant first depends on its intrinsic properties. The potential to create highly charged functional groups, the very small size allowing a close packing of grafted entities and the molecule morphology facilitating the access to adsorption

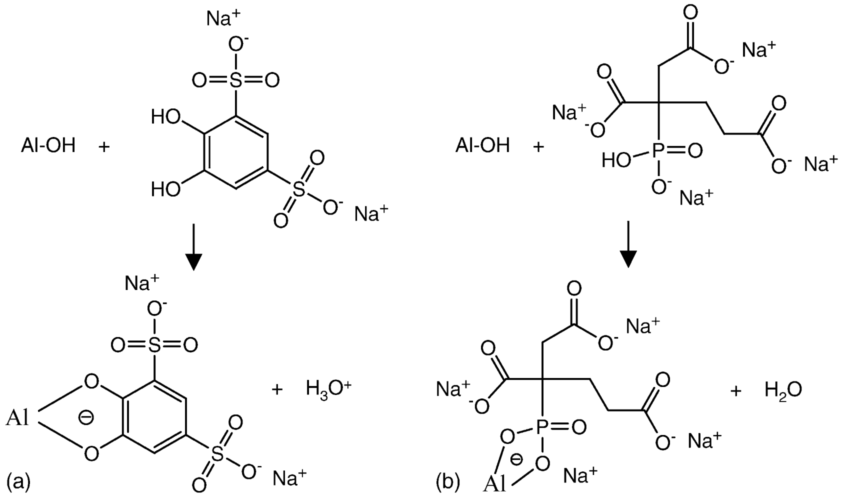

Fig. 7. Adsorption mechanisms of Tiron (a) and PBTCA (b).

sites are beneficial parameters. But, the real effectiveness may vary a lot depending on the surface chemistry of raw alumina ultrafine powders in solution, more specifically the hydroxylation and ionisation of Al–OH groups, that control the number as well as the accessibility of adsorption sites.

The adsorption of Tiron is known to be due to the formation of an inner sphere complex between the alcohol groups of the Tiron molecule and the metal ion of the alumina surface (Fig. 7a). For a mixed carboxylate-phosphonate molecule, such as PBTCA, it has been demonstrated that the substitution of COO^- by $PO_3{}^{2-}$ increases the stability of complexes with Al(III) because of the higher basicity of phosphonic groups, even if the higher spatial requirements of phosphonic function and the greater electrostatic repulsion may overcompensate this effect.[20] We think that the grafting mechanism of PBTCA on alumina surface is most likely linked to the affinity of the phosphonate *foot* for hydroxylic groups also through the creation of an inner sphere complex by ligand exchange process (Fig. 7b). In order to verify this assumption, we have carried out ESA measurements using butane-1,2,4-tricarboxylic acid (BTCA). In that case, we can not observe any IEP shift (Fig. 5d) in comparison with pure AKP powders (Fig. 5a). It suggests that there is likely no strong grafting of BTCA on the alumina surface because of the absence of the phosphonate *foot*.

3.5. Adsorption

Adsorption isotherms have been measured for different pH and on a large range of PBTCA concentration for the AKPs and the B15CR powders. The trends are similar for these three powders and only the results with AKP30 are presented (Fig. 8a) in comparison with adsorption isotherms of Tiron already published (Fig. 8b).[10,13] Fig. 8a and b show that PBTCA and Tiron behaviours are similar. The added dispersants are first entirely adsorbed until their concentration reaches a value above which no more adsorption happens, i.e. plateau. It most likely indicates that only

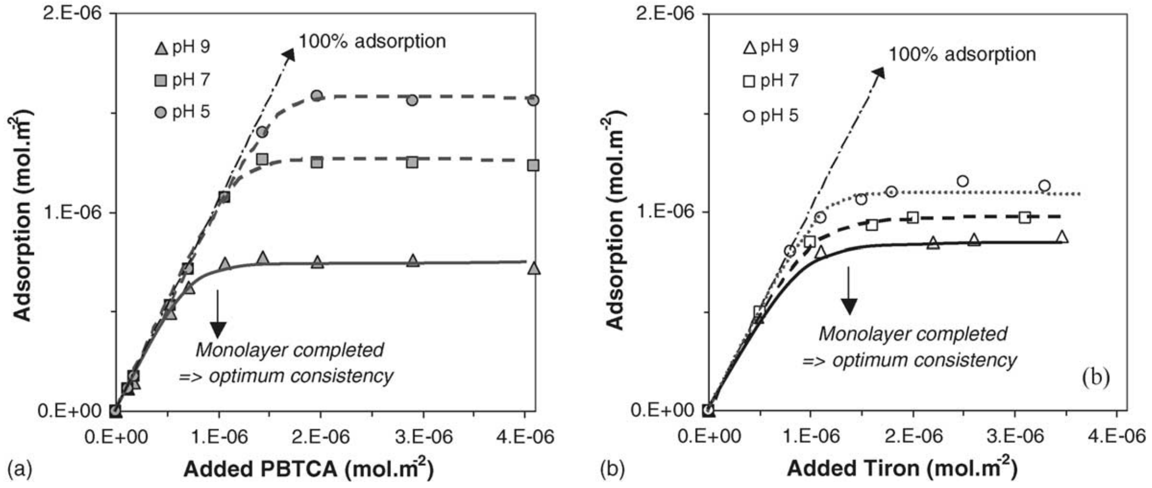

Fig. 8. Adsorption isotherms of PBTCA (a) and Tiron (b) dispersants for the AKP30 powder.

monolayers of Tiron and PBTCA are formed. When there are no more free and accessible adsorption sites, dispersants remain in the solvent acting as weak acids lowering the pH and increasing the ionic strength. At high pH (pH 9 is close to the natural pH of alumina), the plateau starts at concentrations of $10^{-6}\,\mathrm{mol\,m^{-2}}$ and $1.3 \times 10^{-6}\,\mathrm{mol\,m^{-2}}$ for PBTCA and Tiron, respectively, which also leads to minimum consistency for concentrated suspensions (Fig. 4). This corresponds to molar concentrations of additives of the order of 1000 ppm with respect to the alumina content. The authors are aware that this may be a problem to limit abnormal grain growth during sintering stage, more specifically in the presence of Na, and an additional work is in progress to replace Na counter-ions with ammonium ones. At pH 5, the Tiron concentration corresponding to the beginning of the plateau remains unchanged, whereas it rises up to $1.8 \times 10^{-6}\,\mathrm{mol\,m^{-2}}$ for PBTCA. This is likely due to the neutralization of some of the carboxylic groups of PBTCA, that reduces repulsive forces between grafted molecules and leads to a better packing of them. As already observed by Liu et al.[11] for PBTCA and Laucournet et al.[13] for Tiron, the quantity of adsorbed dispersant decreases when pH increases. This is due to the electrostatic repulsion between the negative charges localized at the powder surface and the negatively charged dispersant molecules. In addition, the number of positively charged sites on alumina surface, where PBTCA and Tiron molecules are likely to adsorb, decreases at high pH. Finally, it should be noted that the adsorption of Tiron is less sensitive to the variation of pH than the PBTCA one. The progressive neutralization of the carboxylic groups of PBTCA at pH ranging from 6.8 down to 4.23 is probably of major influence since it promotes a close packing of grafted molecules. A calculation using Chem3D from CambridgeSoft also shows that the negative partial charge in the neighbourhood of the phosphonate foot of PBTCA is higher than that around the hydroxyl groups of Tiron (Fig. 2). As a result, the influence of electrostatic forces on the grafting of dispersants onto charged alumina surface might be lower with Tiron. In comparison, the grafting of PBTCA would be improved at low pH (i.e. alumina surface positively charged) and inhibited at high pH (i.e. alumina surface negatively charged) as observed in Fig. 8.

3.6. Implementation of DCC process

The demonstration of the effectiveness of some of the studied suspensions in the DCC process through to the finished product has been done. The AKP30 powder was chosen because of the possibility to reach the highest solid loading together with viscosities compatible with degassing and casting. An AKP30 dispersion, with a solid loading of 57.5 vol.%, dispersed using an optimum concentration of PBTCA dispersant, exhibits a viscosity of 0.18 Pa s at a shear rate of $100\,\mathrm{s^{-1}}$. The coagulation of such a dispersion can be easily obtained by shifting the pH towards the IEP. The coagulant can be similar to that used by Prabhakaran et al.[21] to get stiff pastes. The degassing of the suspension is performed under slow agitation to promote the release of the bubbles. It is done before the coagulant is introduced. The coagulant is added at an optimum concentration to the degassed suspension while taking care not to create bubbles. The suspension is poured in a Teflon non-porous mould. Finally the coagulation takes place within few minutes depending on the processing temperature and composition of the coagulant. The study of the coagulation kinetics with respect to the temperature and composition will be presented in a forthcoming paper. Anyway, the first results obtained are promising. The density of granular compacts after drying have been measured to be nearly 60 vol.%. The distribution of the pore diameter, measured by mercury porosimetry, is centred on 100 nm with a low standard deviation of about 50 nm (Fig. 9a). This indicates a very homogeneous staking of particles as shown in Fig. 9b, that validates the DCC

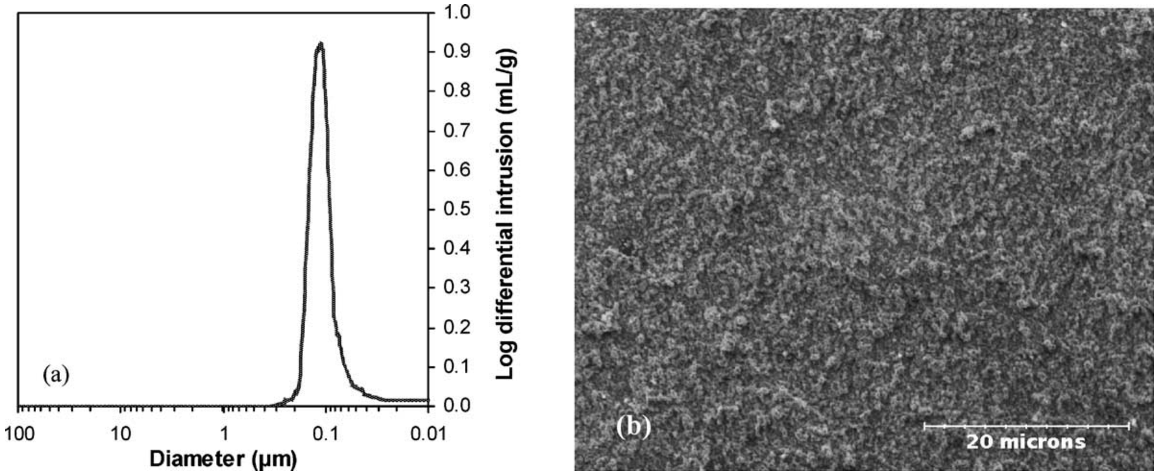

Fig. 9. DCC on 57.5 vol.% AKP 30 suspensions initially stabilized with PBTCA. Typical diameter of pores after drying of coagulated bodies (a) and SEM image of particles stacking (b).

process and more specifically the degassing procedure. Complex parts have been shaped this way.

4. Conclusion

The studies of consistency, surface charging and adsorption isotherms allow the conclusion that PBTCA is as effective as Tiron, and hence a good alternative for the aqueous dispersion of alumina ultrafine particles. The adsorption of PBTCA and Tiron results from similar mechanisms. Both molecules are grafted as monolayers through the creation of inner sphere complexes by ligand exchange processes. The alumina surface chemistry, and more specifically the hydroxylation, regulates the adsorption through the number of adsorption sites it permits. Further studies, such as colloidal force measurements, are in progress to better characterize this surface chemistry. Moreover, the alumina surface charging with PBTCA is more sensitive to pH variations than with Tiron. Preliminary experiments confirm the conclusions presented in this paper showing that PBTCA is a suitable dispersant for the implementation of a simple, fast and reliable DCC shaping process.

Acknowledgements

Baikowski SA (France) for supplying free samples of B15 CR alumina.

References

1. Mayo, M. J., Nanoceramic toys. *Adv. Eng. Mater.* 2000, **2**, 409–415.
2. Krell, A., Pippel, E., Woltersdorf, J. and Burger, W., Subcritical crack growth in Al_2O_3 with submicron grain size. *J. Eur. Ceram Soc.* 2003, **23**, 81–89.
3. Lange, F. F., Powder processing science and technology for increased reliability. *J. Am. Ceram. Soc.* 1989, **72**(1), 3–15.
4. Lewis, J. A., Colloidal processing of ceramics. *J. Am. Ceram. Soc.* 2000, **83**(10), 2341–2359.
5. Bowen, P. and Carry, C., From powders to sintered pieces: forming, transformations and sintering of nanostructured ceramic oxides. *Powder Technol.* 2002, **128**, 248–255.
6. Krell, A., Blank, P., Ma, H., Hutzler, T. and Nebelung, M., Processing of high-density submicrometer Al_2O_3 for new applications. *J. Am. Ceram. Soc.* 2003, **86**(4), 546–553.
7. Omatete, O. O., Janney, M. A. and Strehlow, R. A., Gelcasting—a new ceramic forming process. *Am. Ceram. Soc. Bull.* 1991, **70**(10), 1641–1649.
8. Young, A. C., Omatete, O. O., Janney, M. A. and Menchhofer, P. A., Gelcasting of alumina. *J. Am. Ceram. Soc.* 1991, **74**(3), 612–618.
9. Gaukler, L. J., Graule, Th. and Baader, F., Ceramic forming using enzyme catalyzed reactions. *Mater. Chem. Phys.* 1999, **61**, 78–102.
10. Laucournet, R., Pagnoux, C., Chartier, T. and Baumard, J. F., Coagulation method of aqueous concentrated alumina suspensions by thermal decomposition of hydroxyaluminum diacetate. *J. Am. Ceram. Soc.* 2000, **83**(11), 2661–2667.
11. Liu, Y. Q., Gao, L., Yu, L. and Guo, J., Adsorption of PBTCA on alumina surfaces and its influence on the fractal characteristics of sediments. *J. Colloid Interf. Sci.* 2000, **227**(1), 164–170.
12. Studart, A. R., Pandolfelli, V. C., Tervoort, E. and Gauckler, L. J., Selection of dispersants for high-alumina zero-cement refractory castables. *J. Eur. Ceram. Soc.* 2003, **23**, 997–1004.
13. Laucournet, R., Pagnoux, C., Chartier, T. and Baumard, J. F., Catechol derivatives and anion adsorption onto alumina surfaces in aqueous media: influence of the electrokinetic properties. *J. Eur. Ceram. Soc.* 2001, **21**, 869–878.
14. Liu, Y. Q., Gao, L. and Guo, J., Comparative study of the stabilizing effect of 2-phosphonobutane-1,2,4-tricarboxylic acid and citric acid for alumina suspensions. *Colloids Surf. A* 2001, **193**, 187–195.
15. Liu, Y. and Gao, L., Deflocculation study of aqueous nanosized Y-TZP suspensions. *Mater. Chem. Phys.* 2002, **78**, 480–485.
16. Liu, Y. and Gao, L., Effect of 2-phosphonobutane-1,2,4-tricarboxylic acid adsorption on the stability and rheological properties of aqueous nanosized 3-mol%-Yttria-stabilized tetragonal-zirconia polycrystal suspensions. *J. Am. Ceram. Soc.* 2003, **86**, 1106–1113.
17. Drela, I., Falewicz, P. and Kuczkowska, S., New rapid test for evaluation of scale inhibitors. *Water Res.* 1998, **32**, 3188–3191.
18. Briscoe, B. J., Khan, A. U. and Luckham, P. F., Optimising the dispersion on an alumina suspension using commercial polyvalent electrolyte dispersants. *J. Eur. Ceram. Soc.* 1998, **18**, 2141–2147.
19. Hidber, P. C., Graule, T. J. and Gauckler, L. J., Influence of the dispersant structure on properties of electrostatically stabilized aqueous alumina suspensions. *J. Eur. Ceram. Soc.* 1997, **17**, 239–249.
20. Rubini, P., Lakatos, A., Champmartin, D. and Kiss, T., Speciation and structural aspects of interactions of Al(III) with small biomolecules. *Coord. Chem. Rev.* 2002, **228**, 137–152.
21. Prabhakaran, K., Ananthakumar, S. and Pavithran, C., Preparation of extrudable alumina paste by coagulation of electrosterically stabilized aqueous slurries. *J. Eur. Ceram. Soc.* 2002, **22**, 153–158.